ISSN 0915-633X

NATIONAL INSTITUTE FOR FUSION SCIENCE

Identification of Tubular Vortices in Complex Flows

H. Miura and S. Kida

(Received - Oct. 28, 1996)

NIFS-466 Dec. 1996

RESEARCH REPORT
NIFS Series

NAGOYA, JAPAN

Identification of Tubular Vortices in Complex Flows

Hideaki MIURAand Shigeo KIDA
Theory and Computer Simulation Center,
National Institute for Fusion Science,Nagoya 464-01

Abstract

A new method is proposed to extract the axes of tubular vortices in complex fluid flows. Loci of sectional local minimum of the pressure associated with the advection acceleration are traced numerically. It is applied to a homogeneous isotropic turbulence to demonstrate that swirling motions actually exist around these axes. The present method is shown to be superior to several typical ones commonly used in identifying tubular vortices.

KEYWORDS: identification of vortices, tubular vortices, turbulence, sectionally local minimum

I. INTRODUCTION

Characterization and extraction of coherent structures, such as vortex tubes and layers, are prerequisite for the study of turbulence dynamics. In a homogeneous shear turbulence, for example, several typical complex interactions are observed between vortex tubes and layers.[1] It is not easy, however, to identify tubular vortices accompanied with swirling motions around them because vorticity does not necessarily bring about a swirling motion. Many identification methods have been proposed so far in terms of regions of high vorticity, high strain, low pressure, topological structures of streamlines and streaklines, sectional concave regions of pressure, and so on (see Ref. 2 for a review). Unfortunately, however, we must admit that none of them can capture swirling motions in turbulence objectively and satisfactorily. Some methods have artificial adjustable parameters and others mispredict swirling motions.

In this paper, we propose a new method to extract the axes of tubular vortices in complex flows. In § 2, we characterize a tubular vortex in terms of the pressure associated with the advection acceleration and explain how to trace their axes. In § 3, we show that our method is superior to others in identification of the axes of tubular vortices in homogeneous turbulence. Section 4 is devoted to further discussions.

II. SECTIONALLY MINIMAL PRESSURE METHOD

We consider here how to extract tubular vortices, or swirling slender regions, in complex flows. For characterization of a tubular vortex, it may be useful to recall the fact that the pressure is generally lower inside a vortex than the surroundings to counter-balance the centrifugal force due to swirling motions around it. More precisely, the pressure takes a minimum value around the central axis in a cross-section of a vortex.[2] We may call it the sectionally local minimum of the pressure. In a given velocity field $\boldsymbol{u}(\boldsymbol{x})$ each fluid element feels advective acceleration $(\boldsymbol{u}\cdot\nabla)\boldsymbol{u}$.[3] A force field associated with this advection acceleration, which maintains the velocity field stationarily, is generally expressed as the sum of a potential force and a torque as

$$(\boldsymbol{u}\cdot\nabla)\boldsymbol{u} = -\nabla P + \nabla\times\boldsymbol{Q}. \tag{1}$$

Here, P and $\boldsymbol{Q}$ are completely determined within constants by an instantaneous velocity field $\boldsymbol{u}(\boldsymbol{x})$ under an appropriate boundary condition. Scalar potential P obeys the Poisson equation

$$\nabla^2 P = -\frac{\partial^2}{\partial x_i \partial x_j}(u_i u_j) \tag{2}$$

for an incompressible flow, which follows from eq.(1) by taking a divergence of it. Equation (2) is identical to the equation of the pressure for an incompressible Newtonian fluid flow without any external torques, in which P coincides with the true pressure. Scalar potential P introduced in eq.(1) may be called the pressure associated with the advection acceleration. Based on the above observation of the low pressure in a tubular vortex, we define here the axis of a vortex as a locus of sectionally local minimum of the pressure associated with the advection acceleration.

The loci of sectionally local minimum of the pressure is traced numerically as follows. First, we expand the pressure around each grid point (X_1, X_2, X_3) up to the second order as

$$P(x_1, x_2, x_3) = P^{(0)} + P_i^{(1)}(x_i - X_i) + \tfrac{1}{2}P_{ij}^{(2)}(x_i - X_i)(x_j - X_j), \tag{3}$$

where $P^{(0)} = P(X_1, X_2, X_3)$, $P_i^{(1)} = (\partial/\partial X_i)P(X_1, X_2, X_3)$ and $P_{ij}^{(2)} = (\partial^2/\partial X_i \partial X_j)$ $P(X_1, X_2, X_3)$. Next, this quadratic form is transformed into a normal form

$$P = P_{min} + \tfrac{1}{2}\lambda^{(i)}\,(x_i' - c_i)^2 \tag{4}$$

by a rotation around the origin of the coordinate system from (x_1, x_2, x_3) to (x_1', x_2', x_3'). Here, $\lambda^{(i)}$ $(i = 1, 2, 3)$ are the eigenvalues of pressure hessian $\{P_{ij}^{(2)}\}$. The x_i'-axis is parallel to the eigenvector associated with $\lambda^{(i)}$. Since $\{P_{ij}^{(2)}\}$ is a symmetric tensor, $\lambda^{(i)}$ are real. We assume, without loss of generality, that $\lambda^{(1)} \geq \lambda^{(2)} \geq \lambda^{(3)}$. The condition of a tubular vortex is then given by $\lambda^{(2)} > 0$. The vortex is thought to be parallel to the x_3'-axis if $\lambda^{(3)} < 0$. Then, a foot point, $\boldsymbol{C}'(c_1', c_2', c_3')$ say, of a normal line from the grid point $\boldsymbol{X}$ to a straight line parallel to the x_3'-axis passing through point $\boldsymbol{C}(c_1, c_2, c_3)$ is regarded as lying on the axis of a tubular vortex (see Fig. 1).

It should be noticed that the above quadratic approximation of the pressure may be valid only if the distance between the axial point $\boldsymbol{C}'$ and the grid point $\boldsymbol{X}$ is sufficiently small. The critical length may be different depending upon the velocity field. For example, this approximation may be poor where two vortices are close each other. Except for such rather rare regions, we assume that it may be permissible if $|\boldsymbol{X} - \boldsymbol{C}|$ is less than of order of mesh-size δ (a minimum length available in a numerical data) in a regular grid system which we analyze in the following. It should also be noticed that plural neighboring grid points may predict same loci of local minimum of pressure with small difference, which may lead to redundant predictions. To avoid such redundancy, we discard all the points other than that predicted from a grid point nearest to the locus. Practically, we take only such points that satisfy the condition that $\lambda^{(2)} > 0$ and $|X_i - c_i'| < \frac{1}{2}\delta$ $(i = 1, 2, 3)$. Each point is then connected with its nearest-neighbor within two mesh-sizes in each coordinate axis to construct the axial lines of tubular vortices.

The vortex-axis-tracing method described above is applied to a homogeneous isotropic turbulence of micro-scale Reynolds number 27 which was simulated in a periodic cube with

64^3 grid points. The axes of tubular vortices thus obtained are depicted by strings of tubular pieces in Fig. 2. Colors of the tubes represent the sum of two positive eigenvalues, $\lambda_1 + \lambda_2$ which measure the depth of potential wells and also the strength of vortices. Blue is stronger and yellow is weaker. Typical streamlines which are viewed in frames moving[5] relative to the nearest part of the axes of vortices are drawn with red. It is seen that they coil up around the vortex axes irrespective of strength, implying that there are indeed swirling motions around them.

III. COMPARISON WITH OTHER METHODS

We now compare our new method with some typical identification methods which have been proposed so far, such as the representations with isosurfaces of high enstrophy density $\frac{1}{2}|\omega|^2$, low pressure p, high Laplacian of pressure $\nabla^2 p$ and the λ_2-definition.[2]

Visualization of vortex structures by enstrophy density $\frac{1}{2}|\omega|^2$ has been frequently used in the numerical study of complex flows. In Fig. 3(a), we show the isosurfaces of enstrophy density at the level a half of the standard deviation above the mean value. This level was selected carefully for a better representation. At lower levels more vortices can be included in isosurfaces, but the covered volume is inevitably too large to distinguish the individual vortices. At higher levels, on the other hand, some vortices can be identified more sharply but more vortices are left outside of isosurfaces. In spite of such a deliberate adjustment, some of vortices still remain outside of the isosurfaces in Fig. 3(a). There is an intrinsic difficulty in the representation in terms of isosurfaces of enstrophy density that swirling and shearing motions cannot be distinguished solely by vorticity (see Ref. 4). As is well known, swirling motions are not always realized where intensity of vorticity is high if shearing motions are strong. It should be emphasized that swirling motions exist either inside or outside of isosurfaces of enstrophy density and that our method can capture them even where vorticity is weak.

In Fig. 3(b) drawn are isosurfaces of the pressure, which is expected to be lower at tubular vortices than the surroundings, at the level of a standard deviation below the mean value. This level was again selected deliberately for a better representation. Nevertheless it does not seem to capture the tubular vortices well. Many vortices are indeed enclosed by

isosurfaces of the pressure at this level, but it is not so sharp. Moreover, some axial lines are outside of the isosurfaces. The pressure is not by nature a good indicator of tubular vortices. Indeed it is lower at vortices than the surroundings, but the absolute value depends on the surrounding pressure. The amount of depression of pressure varies depending upon the strength of vortices. Thus it is not surprising that the isosurfaces of pressure may not describe well swirling motions of various strength simultaneously.

Isosurfaces of $\nabla^2 p$, threshold of which is given by a standard deviation above the mean value, are drawn in Fig. 3(c) (see Ref. 4). These isosurfaces capture tubular vortices relatively well in the sense that most of the vortices are covered rather sharply. Although some vortices are still outside of the isosurfaces, the vortex identification by $\nabla^2 p$ seems to be better than previous two in capturing swirling motions. Isosurfaces at the zero levels, which are called the Q-definition,[2] cover too wide regions of the flow field to identify the individual vortices (figures are omitted). We conclude therefore that the Laplacian of pressure may be able to represent the tubular vortices well if the threshold is set appropriately.

Recently, Jeong and Hussain[2] introduced the second eigenvalue λ_2 of symmetric tensor $S_{ik}S_{kj} + \Omega_{ik}\Omega_{kj}$, where S_{ij} and Ω_{ij} are respectively the symmetric and anti-symmetric parts of velocity gradient tensor $\nabla \boldsymbol{u}$, and defined vortex cores by the regions of $\lambda_2 < 0$. This λ_2-definition was successfully applied to several kinds of flows with clear vortical structures. In Fig. 3(d), we show isosurfaces of null-λ_2, which include all of the tubular vortices but cover too much volume to distinguish each. Therefore, this definition may not be suitable to represent tubular vortices in turbulent flows. It should be mentioned, however, that isosurfaces of λ_2 at a lower level give a better representation comparable with isosurfaces of $\nabla^2 p$ in Fig. 3(c).

IV. CONCLUDING REMARKS

The sectionally minimal pressure method to visualize the axes of tubular vortices was proposed and applied successfully to homogeneous turbulence. It was shown that tubular vortices can be captured irrespective of strength. This new method is superior in identification of the axes of tubular vortices to several typical ones proposed before such as the representations by isosurfaces of high enstrophy density, low pressure, high Laplacian of

pressure and the λ_2-definition. In course of this comparison, we found that the Laplacian of the pressure may represent tubular vortices better than others though it has a subjective artifact of an appropriate choice of the threshold level. The λ_2-definition and Δ-definition[2,6], which are free from defining threshold of isosurfaces, were also checked not to represent tubular vortices in a homogeneous turbulence well.

Our method also works well for homogeneous shear turbulence of an incompressible fluid[1,4] as well as for an isotropic compressible turbulence with shock waves. These results will be reported in a separate paper.

We would like to express our cordial gratitude to Drs. S. Kishiba in Hiroshima University and M. Tanaka in Kyoto Institute of Technology for their kind offers of numerical data of turbulent flows in the earlier stage of the present study. We would also like to thank to Drs. K. Araki, A. Kageyama and T.-H. Watanabe in the Complexity Simulation Group in the National Institute for Fusion Science (NIFS) for their technical support for visualization of numerical data. The calculation was carried out on the SX-3 system in the Theory and Computer Simulation Center, NIFS. This work was partially supported by a Grant-in-Aid for Scientific Research from the Ministry of Education, Science and Culture in Japan.

REFERENCES

[1] S. Kida and M. Tanaka "Dynamics of vortical structures in a homogeneous shear flow", J. Fluid Mech. **274** (1994) 43.

[2] J. Jeong and F. Hussain "On the identification of a vortex", J. Fluid Mech. **285** (1995) 69 .

[3] The total acceleration is $\partial \boldsymbol{u}/\partial t + (\boldsymbol{u} \cdot \nabla)\boldsymbol{u}$.

[4] M. Tanaka and S. Kida "Characterization of vortex tubes and sheets", Phys. Fluids A **5** (1993) 2079.

[5] Swirling streamlines are generally not observed in a fixed frame.

[6] M. S. Chong, A. E. Perry and B. J. Cantwell "A general classification of three-dimensional flow fields", Phys. Fluids A **2** (1990) 765.

FIGURES

FIG. 1. Search for a locus of sectionally local minimum of pressure.

FIG. 2. Axes of tubular vortices (blue-yellow) and streamlines (red). Colors of the vortex axes represent the sum of two positive eigenvalues $\lambda_1 + \lambda_2$, where blue denotes larger values and yellow smaller. The streamlines are drawn in moving frames relative to the nearest part of the vortex axes.

FIG. 3. (a) Isosurfaces of the enstrophy density at the level of a half of standard deviation above the mean. (b) Isosurfaces of the pressure at the level of a standard deviation below the mean. (c) Isosurfaces of $\nabla^2 p$ at the level of a standard deviation above the mean. (d) Isosurfaces of λ_2-definition. Tubular pieces are same as those in Fig. 2.

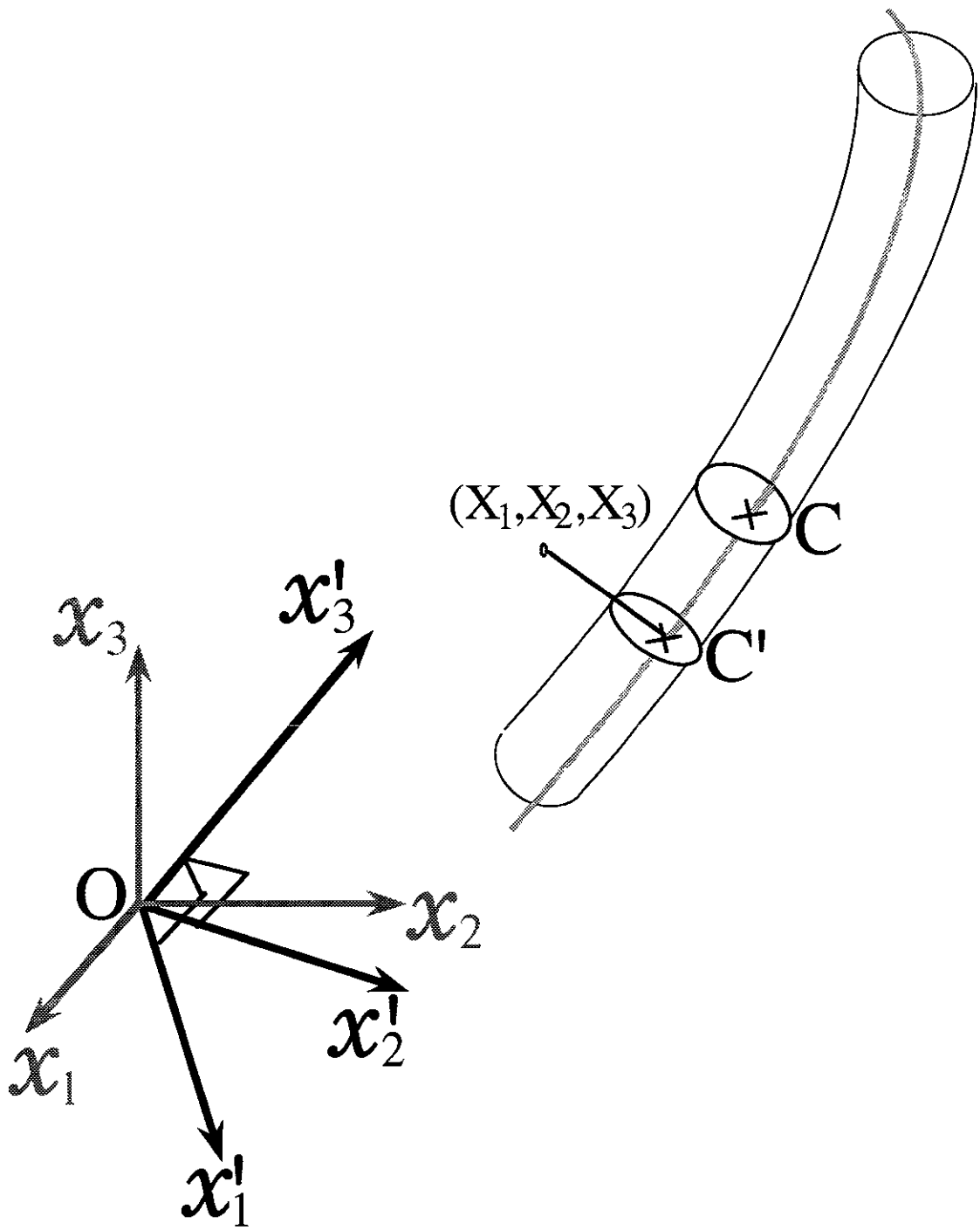

FIG. 1.

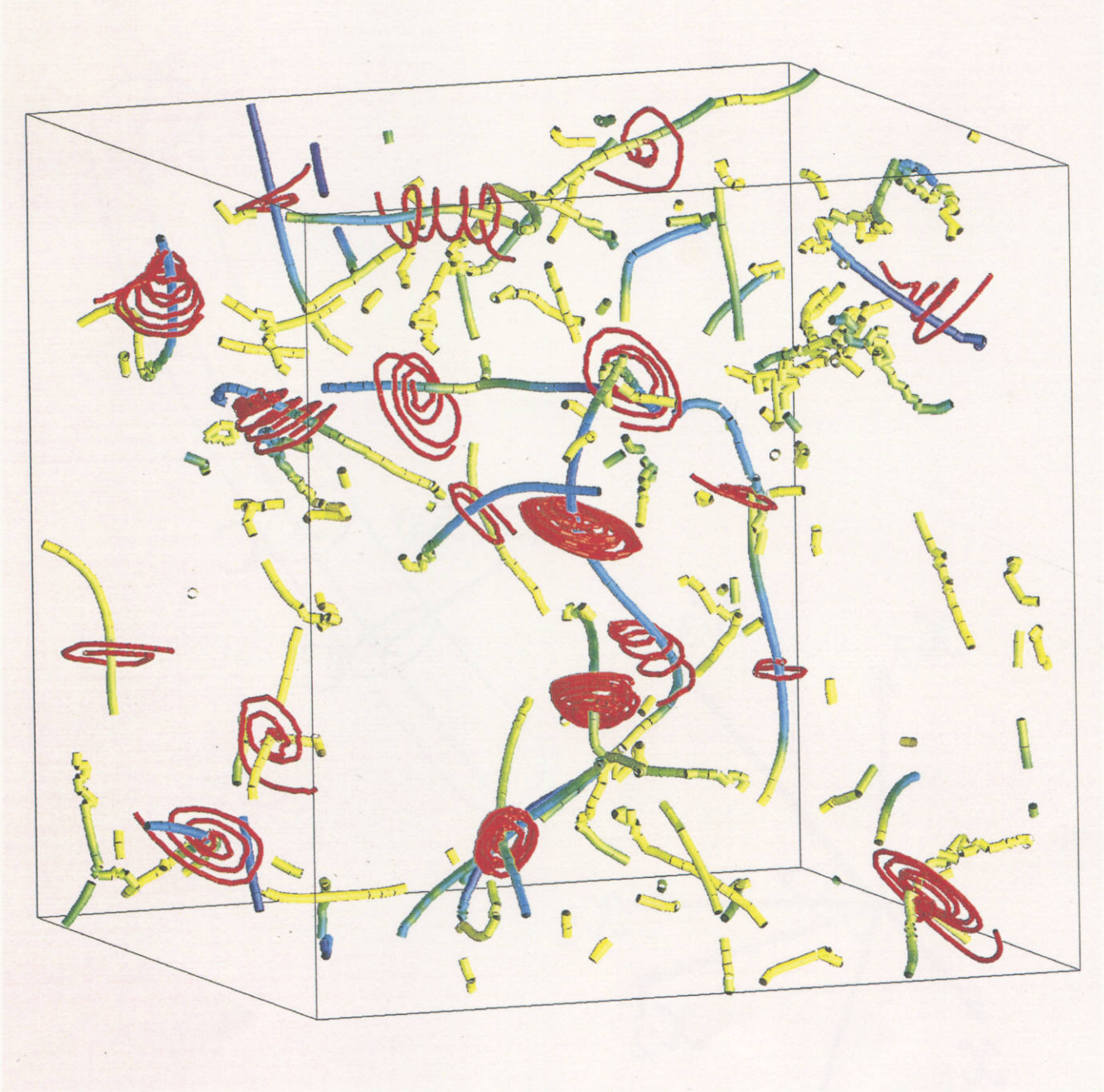

FIG. 2.

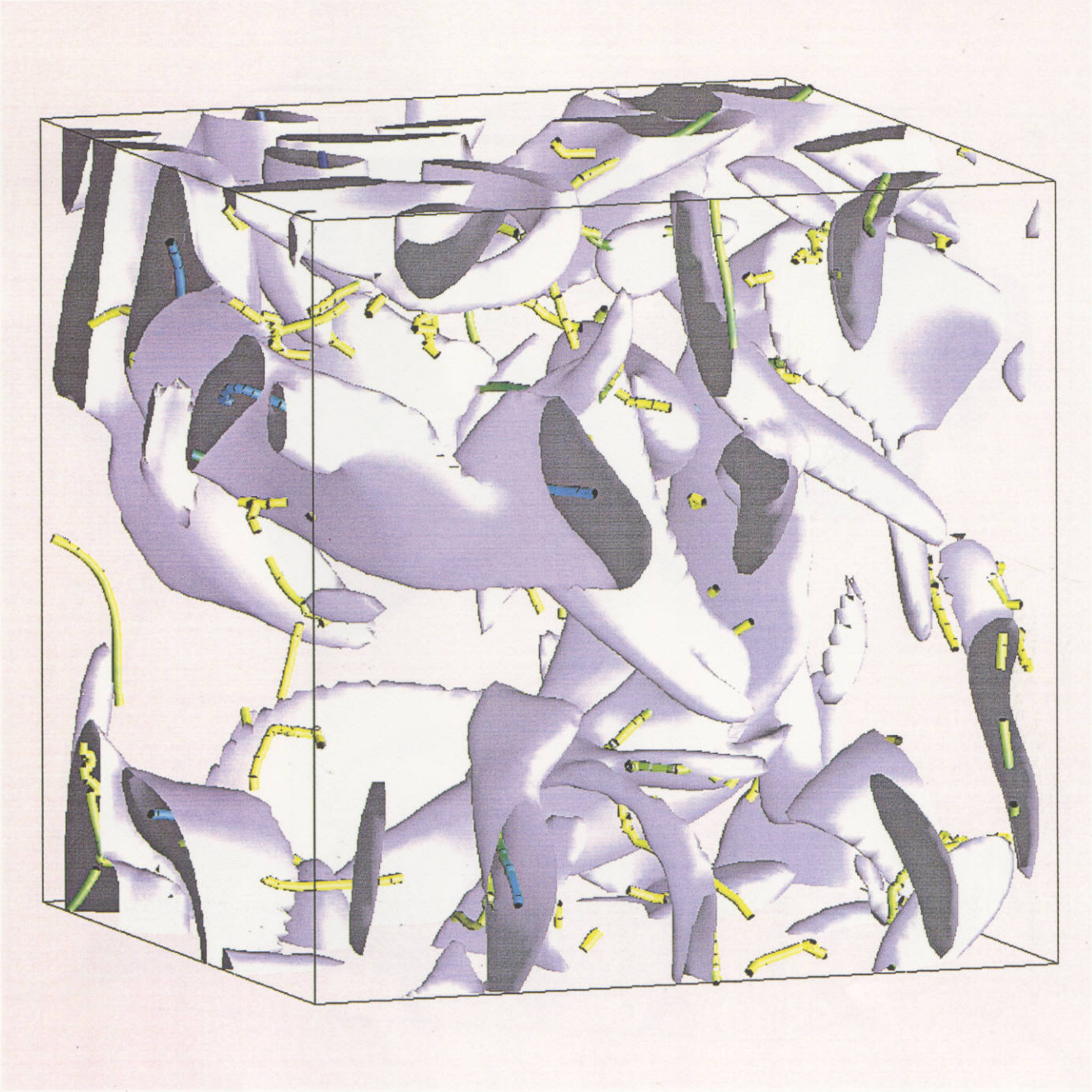

FIG. 3. (a)

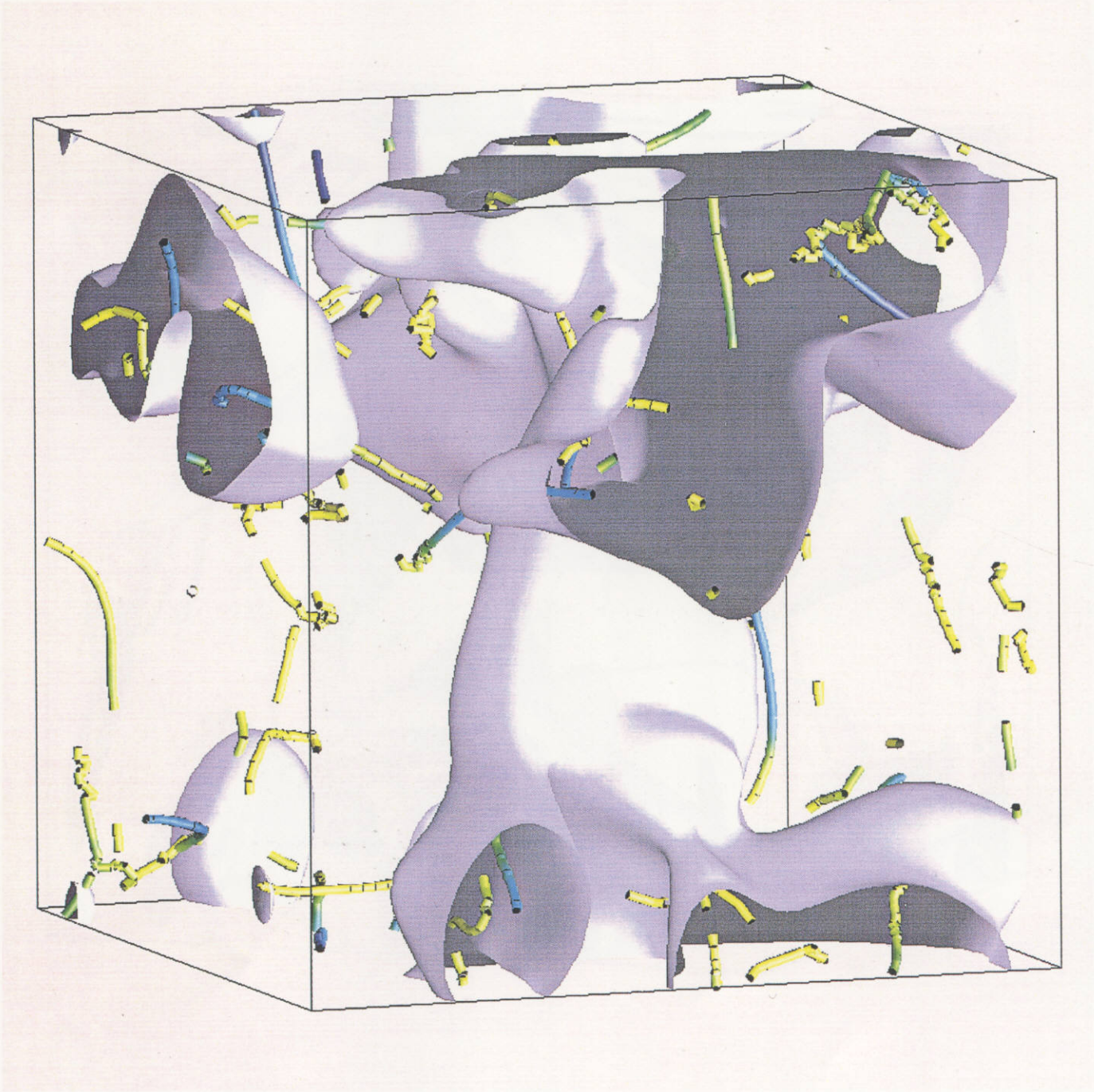

FIG. 3. (b)

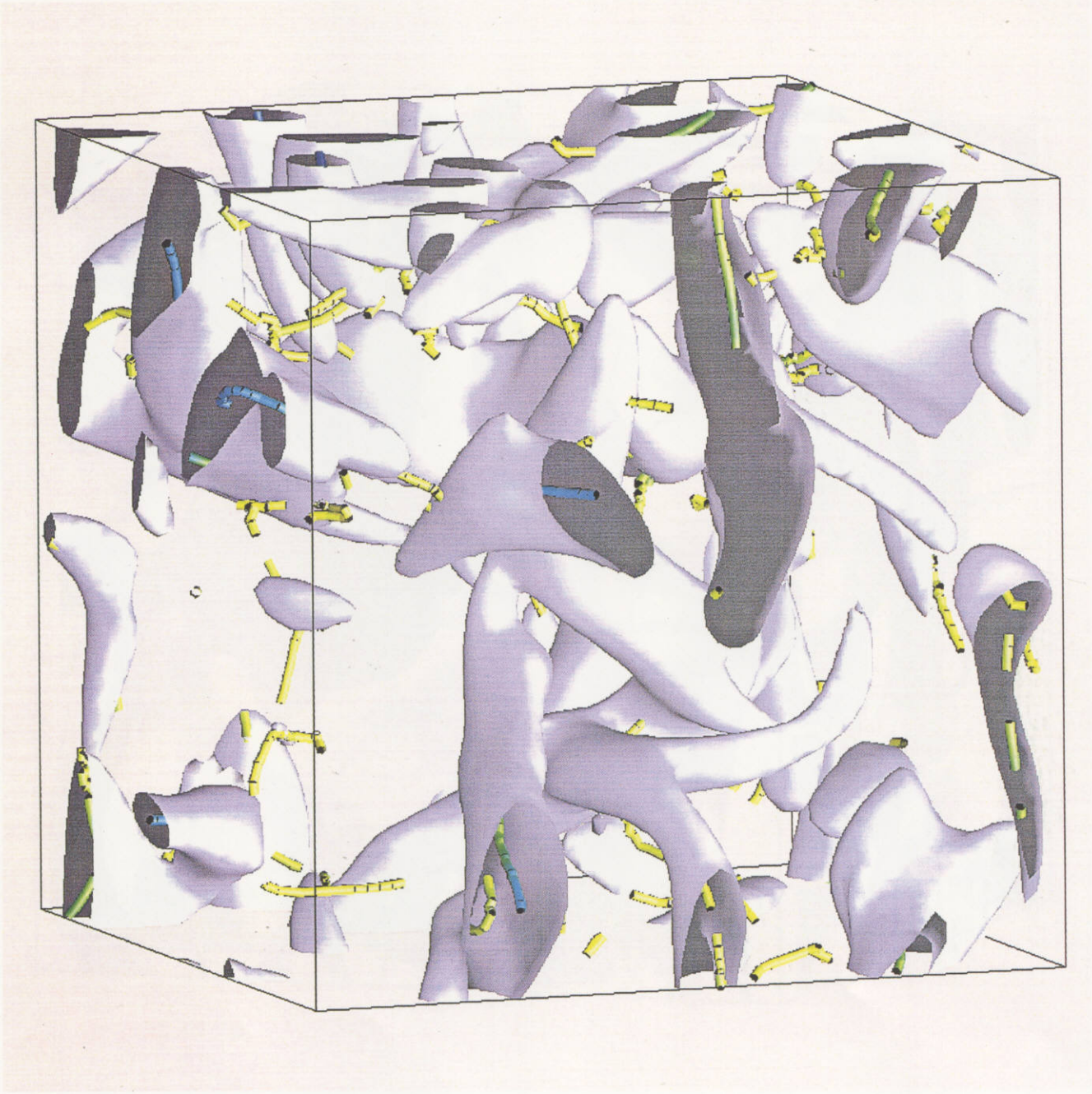

FIG. 3. (c)

FIG. 3. (d)

Recent Issues of NIFS Series

NIFS-427 S. Kida and S. Goto,
Lagrangian Direct-interaction Approximation for Homogeneous Isotropic Turbulence; July 1996

NIFS-428 V.Yu. Sergeev, K.V. Khlopenkov, B.V. Kuteev, S. Sudo, K. Kondo, F. Sano, H. Zushi, H. Okada, S. Besshou, T. Mizuuchi, K. Nagasaki, Y. Kurimoto and T. Obiki,
Recent Experiments on Li Pellet Injection into Heliotron E; Aug. 1996

NIFS-429 N. Noda, V. Philipps and R. Neu,
A Review of Recent Experiments on W and High Z Materials as Plasma-Facing Components in Magnetic Fusion Devices; Aug. 1996

NIFS-430 R.L. Tobler, A. Nishimura and J. Yamamoto,
Design-Relevant Mechanical Properties of 316-Type Stainless Steels for Superconducting Magnets; Aug. 1996

NIFS-431 K. Tsuzuki, M. Natsir, N. Inoue, A. Sagara, N. Noda, O. Motojima, T. Mochizuki, T. Hino and T. Yamashina.
Hydrogen Absorption Behavior into Boron Films by Glow Discharges in Hydrogen and Helium; Aug. 1996

NIFS-432 T.-H. Watanabe, T. Sato and T. Hayashi,
Magnetohydrodynamic Simulation on Co- and Counter-helicity Merging of Spheromaks and Driven Magnetic Reconnection; Aug. 1996

NIFS-433 R. Horiuchi and T. Sato,
Particle Simulation Study of Collisionless Driven Reconnection in a Sheared Magnetic Field; Aug. 1996

NIFS-434 Y. Suzuki, K. Kusano and K. Nishikawa,
Three-Dimensional Simulation Study of the Magnetohydrodynamic Relaxation Process in the Solar Corona. II.; Aug. 1996

NIFS-435 H. Sugama and W. Horton,
Transport Processes and Entropy Production in Toroidally Rotating Plasmas with Electrostatic Turbulence; Aug. 1996

NIFS-436 T. Kato, E. Rachlew-Källne, P. Hörling and K.-D Zastrow,
Observations and Modelling of Line Intensity Ratios of OV Multiplet Lines for 2s3s 3S1 - 2s3p 3Pj; Aug. 1996

NIFS-437 T. Morisaki, A. Komori, R. Akiyama, H. Idei, H. Iguchi, N. Inoue, Y. Kawai, S. Kubo, S. Masuzaki, K. Matsuoka, T. Minami, S. Morita, N. Noda, N. Ohyabu, S. Okamura, M. Osakabe, H. Suzuki, K. Tanaka, C. Takahashi, H. Yamada, I. Yamada and O. Motojima,
Experimental Study of Edge Plasma Structure in Various Discharges on

Compact Helical System; Aug. 1996

NIFS-438 A. Komori, N. Ohyabu, S. Masuzaki, T. Morisaki, H. Suzuki, C. Takahashi, S. Sakakibara, K. Watanabe, T. Watanabe, T. Minami, S. Morita, K. Tanaka, S. Ohdachi, S. Kubo, N. Inoue, H. Yamada, K. Nishimura, S. Okamura, K. Matsuoka, O. Motojima, M. Fujiwara, A. Iiyoshi, C. C. Klepper, J.F. Lyon, A.C. England, D.E. Greenwood, D.K. Lee, D.R. Overbey, J.A. Rome, D.E. Schechter and C.T. Wilson,
Edge Plasma Control by a Local Island Divertor in the Compact Helical System; Sep. 1996 (IAEA-CN-64/C1-2)

NIFS-439 K. Ida, K. Kondo, K. Nagaski T. Hamada, H. Zushi, S. Hidekuma, F. Sano, T. Mizuuchi, H. Okada, S. Besshou, H. Funaba, Y. Kurimoto, K. Watanabe and T. Obiki,
Dynamics of Ion Temperature in Heliotron-E; Sep. 1996 (IAEA-CN-64/CP-5)

NIFS-440 S. Morita, H. Idei, H. Iguchi, S. Kubo, K. Matsuoka, T. Minami, S. Okamura, T. Ozaki, K. Tanaka, K. Toi, R. Akiyama, A. Ejiri, A. Fujisawa, M. Fujiwara, M. Goto, K. Ida, N. Inoue, A. Komori, R. Kumazawa, S. Masuzaki, T. Morisaki, S. Muto, K. Narihara, K. Nishimura, I. Nomura, S. Ohdachi, M.. Osakabe, A. Sagara, Y. Shirai, H. Suzuki, C. Takahashi, K. Tsumori, T. Watari, H. Yamada and I. Yamada,
A Study on Density Profile and Density Limit of NBI Plasmas in CHS; Sep. 1996 (IAEA-CN-64/CP-3)

NIFS-441 O. Kaneko, Y. Takeiri, K. Tsumori, Y. Oka, M. Osakabe, R. Akiyama, T. Kawamoto, E. Asano and T. Kuroda,
Development of Negative-Ion-Based Neutral Beam Injector for the Large Helical Device; Sep. 1996 (IAEA-CN-64/GP-9)

NIFS-442 K. Toi, K.N. Sato, Y. Hamada, S. Ohdachi, H. Sakakita, A. Nishizawa, A. Ejiri, K. Narihara, H. Kuramoto, Y. Kawasumi, S. Kubo, T. Seki, K. Kitachi, J. Xu, K. Ida, K. Kawahata, I. Nomura, K. Adachi, R. Akiyama, A. Fujisawa, J. Fujita, N. Hiraki, S. Hidekuma, S. Hirokura, H. Idei, T. Ido, H. Iguchi, K. Iwasaki, M. Isobe, O. Kaneko, Y. Kano, M. Kojima, J. Koog, R. Kumazawa, T. Kuroda, J. Li, R. Liang, T. Minami, S. Morita, K. Ohkubo, Y. Oka, S. Okajima, M. Osakabe, Y. Sakawa, M. Sasao, K. Sato, T. Shimpo, T. Shoji, H. Sugai, T. Watari, I. Yamada and K. Yamauti,
Studies of Perturbative Plasma Transport, Ice Pellet Ablation and Sawtooth Phenomena in the JIPP T-IIU Tokamak; Sep. 1996 (IAEA-CN-64/A6-5)

NIFS-443 Y. Todo, T. Sato and The Complexity Simulation Group,
Vlasov-MHD and Particle-MHD Simulations of the Toroidal Alfvén Eigenmode; Sep. 1996 (IAEA-CN-64/D2-3)

NIFS-444 A. Fujisawa, S. Kubo, H. Iguchi, H. Idei, T. Minami, H. Sanuki, K. Itoh, S. Okamura, K. Matsuoka, K. Tanaka, S. Lee, M. Kojima, T.P. Crowley, Y. Hamada, M. Iwase, H. Nagasaki, H. Suzuki, N. Inoue, R. Akiyama, M. Osakabe, S. Morita, C. Takahashi, S. Muto, A. Ejiri, K. Ida, S. Nishimura, K. Narihara, I. Yamada,

K. Toi, S. Ohdachi, T. Ozaki, A. Komori, K. Nishimura, S. Hidekuma, K. Ohkubo, D.A. Rasmussen, J.B. Wilgen, M. Murakami, T. Watari and M. Fujiwara.
An Experimental Study of Plasma Confinement and Heating Efficiency through the Potential Profile Measurements with a Heavy Ion Beam Probe in the Compact Helical System; Sep. 1996 (IAEA-CN-64/C1-5)

NIFS-445 O. Motojima, N. Yanagi, S. Imagawa, K. Takahata, S. Yamada, A. Iwamoto, H. Chikaraishi, S. Kitagawa, R. Maekawa, S. Masuzaki, T. Mito, T. Morisaki, A. Nishimura, S. Sakakibara, S. Satoh, T. Satow, H. Tamura, S. Tanahashi, K. Watanabe, S. Yamaguchi, J. Yamamoto, M.Fujiwara and A. Iiyoshi,
Superconducting Magnet Design and Construction of LHD; Sep. 1996 (IAEA-CN-64/G2-4)

NIFS-446 S. Murakami, N. Nakajima, S. Okamura, M. Okamoto and U. Gasparino,
Orbit Effects of Energetic Particles on the Reachable β–Value and the Radial Electric Field in NBI and ECR Heated Heliotron Plasmas: Sep. 1996 (IAEA-CN-64/CP -6) Sep. 1996

NIFS-447 K. Yamazaki, A. Sagara, O. Motojima, M. Fujiwara, T. Amano, H. Chikaraishi, S. Imagawa, T. Muroga, N. Noda, N. Ohyabu, T. Satow, J.F. Wang, K.Y. Watanabe, J. Yamamoto , H. Yamanishi, A. Kohyama, H. Matsui, O. Mitarai, T. Noda, A.A. Shishkin, S. Tanaka and T. Terai
Design Assessment of Heliotron Reactor; Sep. 1996 (IAEA-CN-64/G1-5)

NIFS-448 M. Ozaki, T. Sato and the Complexity Simulation Group,
Interactions of Convecting Magnetic Loops and Arcades; Sep. 1996

NIFS-449 T. Aoki,
Interpolated Differential Operator (IDO) Scheme for Solving Partial Differential Equations; Sep. 1996

NIFS-450 D. Biskamp and T. Sato,
Partial Reconnection in the Sawtooth Collapse; Sep. 1996

NIFS-451 J. Li, X. Gong, L. Luo, F.X. Yin, N. Noda, B. Wan, W. Xu, X. Gao, F. Yin, J.G. Jiang, Z. Wu., J.Y. Zhao, M. Wu, S. Liu and Y. Han,
Effects of High Z Probe on Plasma Behavior in HT-6M Tokamak; Sep. 1996

NIFS-452 N. Nakajima, K. Ichiguchi, M. Okamoto and R.L. Dewar,
Ballooning Modes in Heliotrons/Torsatrons; Sep. 1996 (IAEA-CN-64/D3-6)

NIFS-453 A. Iiyoshi,
Overview of Helical Systems; Sep. 1996 (IAEA-CN-64/O1-7)

NIFS-454 S. Saito, Y. Nomura, K. Hirose and Y.H. Ichikawa,
Separatrix Reconnection and Periodic Orbit Annihilation in the Harper Map; Oct. 1996

NIFS-455 K. Ichiguchi, N. Nakajima and M. Okamoto,

Topics on MHD Equilibrium and Stability in Heliotron / Torsatron; Oct. 1996

NIFS-456 G. Kawahara, S. Kida, M. Tanaka and S. Yanase,
Wrap, Tilt and Stretch of Vorticity Lines around a Strong Straight Vortex Tube in a Simple Shear Flow; Oct. 1996

NIFS-457 K. Itoh, S.- I. Itoh, A. Fukuyama and M. Yagi,
Turbulent Transport and Structural Transition in Confined Plasmas; Oct. 1996

NIFS-458 A. Kageyama and T. Sato,
Generation Mechanism of a Dipole Field by a Magnetohydrodynamic Dynamo; Oct. 1996

NIFS-459 K. Araki, J. Mizushima and S. Yanase,
The Non-axisymmetric Instability of the Wide-Gap Spherical Couette Flow; Oct. 1996

NIFS-460 Y. Hamada, A. Fujisawa, H. Iguchi, A. Nishizawa and Y. Kawasumi.
A Tandem Parallel Plate Analyzer; Nov. 1996

NIFS-461 Y. Hamada, A. Nishizawa, Y. Kawasumi, A. Fujisawa, K. Narihara, K. Ida, A. Ejiri, S. Ohdachi, K. Kawahata, K. Toi, K. Sato, T. Seki, H. Iguchi, K. Adachi, S. Hidekuma. S.Hirokura, K. Iwasaki, T. Ido, M. Kojima. J. Koong, R. Kumazawa, H. Kuramoto, T. Minami, I. Nomura, H. Sakakita, M. Sasao, K.N. Sato, T. Tsuzuki, J. Xu, I. Yamada and T. Watari,
Density Fluctuation in JIPP T-IIU Tokamak Plasmas Measured by a Heavy Ion Beam Probe; Nov. 1996

NIFS-462 N. Katsuragawa, H. Hojo and A. Mase,
Simulation Study on Cross Polarization Scattering of Ultrashort-Pulse Electromagnetic Waves; Nov. 1996

NIFS-463 V. Voitsenya, V. Konovalov, O. Motojima, K. Narihara, M. Becker and B. Schunke,
Evaluations of Different Metals for Manufacturing Mirrors of Thomson Scattering System for the LHD Divertor Plasma; Nov. 1996

NIFS-464 M. Pereyaslavets, M. Sato, T. Shimozuma. Y. Takita, H. Idei, S. Kubo, K. Ohkubo and K. Hayashi,
Development and Simulation of RF Components for High Power Millimeter Wave Gyrotrons; Nov. 1997

NIFS-465 V.S. Voitsenya, S. Masuzaki, O. Motojima, N. Noda and N. Ohyabu,
On the Use of CX Atom Analyzer for Study Characteristics of Ion Component in a LHD Divertor Plasma; Dec. 1996

NIFS-466 H. Miura and S. Kida,
Identification of Tubular Vortices in Complex Flows; Dec. 1996